Advanced Measurement and Modeling Tools for Improved SOFC Cathodes

Jamie R. Wilson, Lilya Dunyushkina, Yunxiang Lu, Stuart B. Adler
University of Washington, Department of Chemical Engineering

SECA Core Technology Program
May, 2004

Acknowledgements

- University of Washington Department of Chemical Engineering
  - **Jamie Wilson** (PhD student)
  - **Lilya Dunyushkina** (IHTE)
  - **Yunxiang Lu** (PhD student)



- Collaborators
  - **Dan Schwartz** (UW Chemical Engineering)
  - Olga Marina (PNNL)
  - Allan Jacobson (University of Houston)
  - Tatsuya Kawada (Tohoku University)

- Support
  - DOE/NETL SECA Core Technology Program
  - NSF
  - Ford Foundation
  - University of Washington Provost Fund

Motivation: How do we identify and improve physical processes limiting cathode performance?

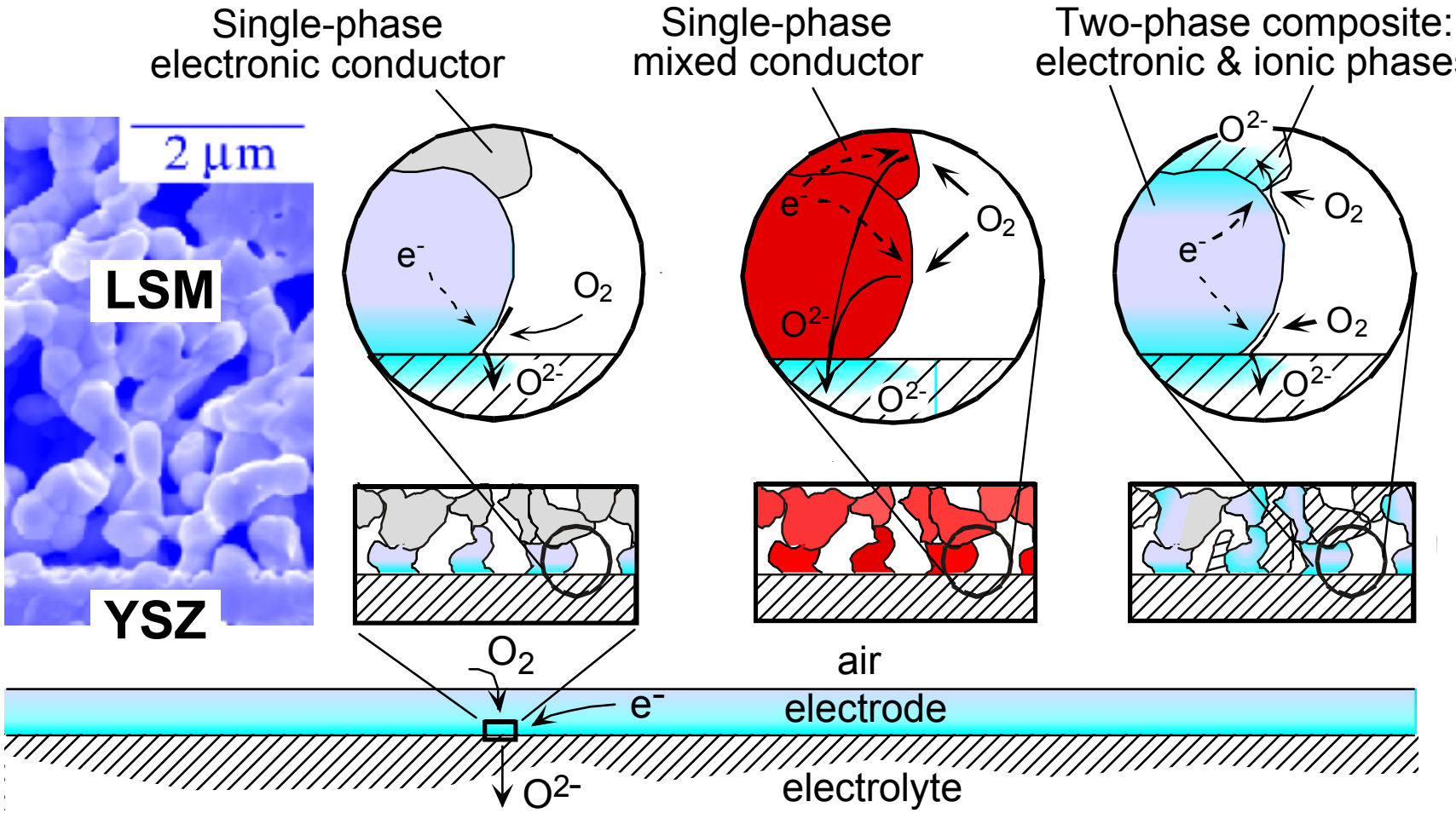

The Problem:

Current electrochemical techniques are limited in the information they can provide.

- Difficult to isolate the performance characteristics of the cathode from the rest of the cell under meaningful conditions.
  - Difficult to implement a reference electrode on a thin electrolyte.
  - Difficult to probe realistic current densities and polarization history.

- Limitations of impedance spectroscopy.
  - Overlap and ambiguity among physical processes (impedance is a “blob”)
  - Lack of physical models linking characteristics to physics.
  - Uniqueness: an inherent limitation of linear response analysis.

Our Approach

- Microelectrodes for improved cathode measurements
  - Better resolution and isolation than standard half-cells.
  - Allows testing of half cells under realistic bias conditions.
- Analysis of nonlinear harmonics (NLEIS, EFM)
  - Helps identify physical processes via. *nonlinearity*.
  - Broader spectrum of information without more experiments.
  - Stronger link between measurements and physical models.

Materials of Interest

Porous Perovskite Electrodes:

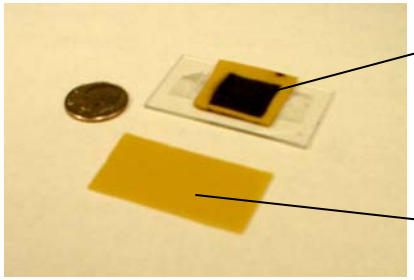

electrode
$La_{1-x}Sr_x(Co,Fe)O_{3-\delta}$

electrolyte
$Ce_{0.8}Sm_{0.2}O_{2-x}$

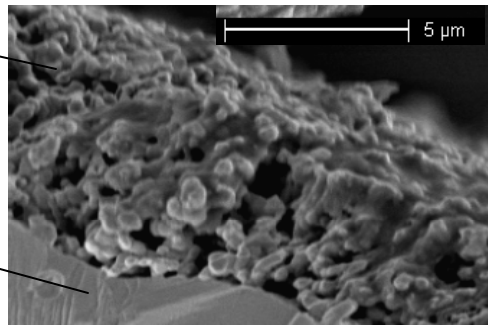

Thin-Film and patterned electrodes:

$La_{0.5}Sr_{0.5}CoO_{3-d}$
on single-crystal YSZ

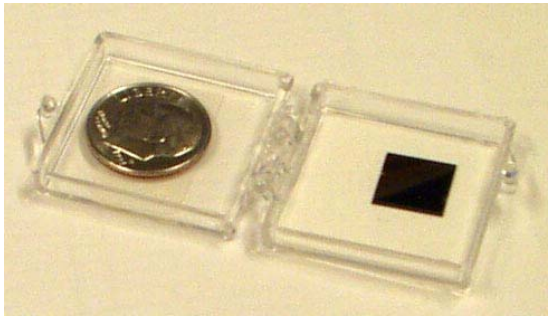

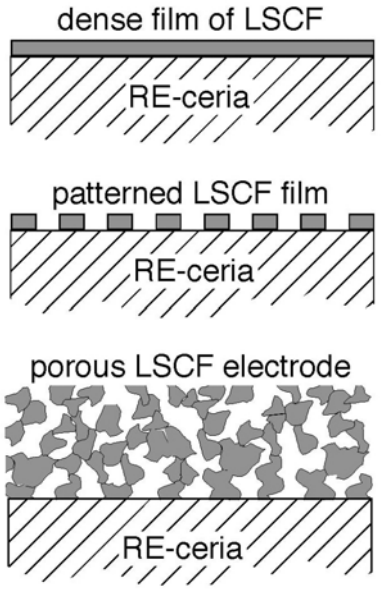

Purpose of a half-cell measurement

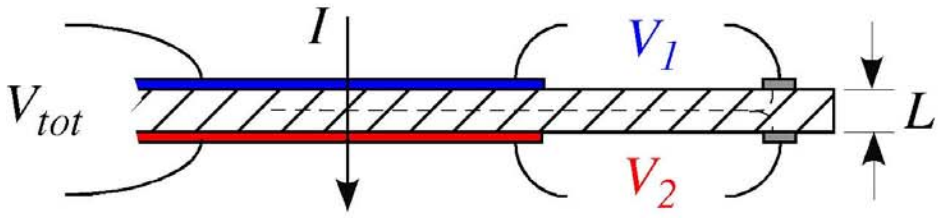

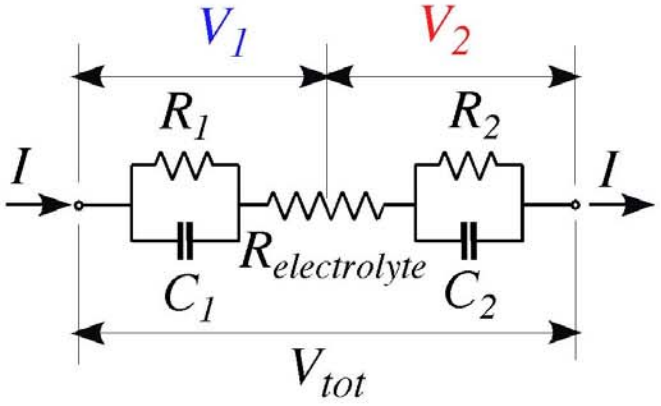

Typical Experimental Goals:

- Measure voltage loss associated with a particular electrode in an operating fuel cell.
- Test electrode at a specific polarization (and history) in a particular environment.
- Isolate the electrode frequency response (impedance).

Reference Electrodes are Prone to Error on Thin Cells

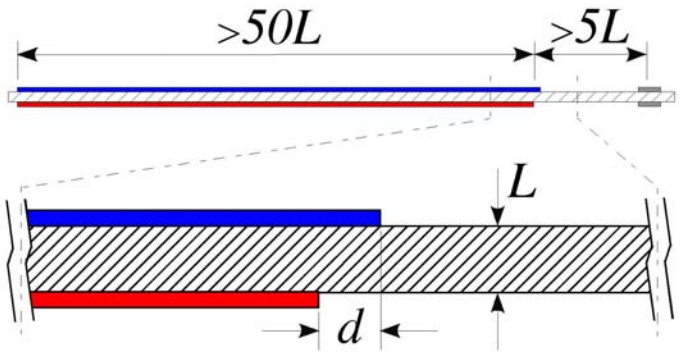

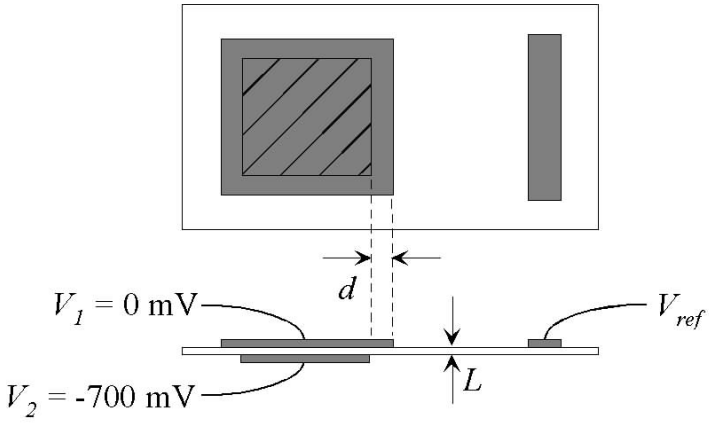

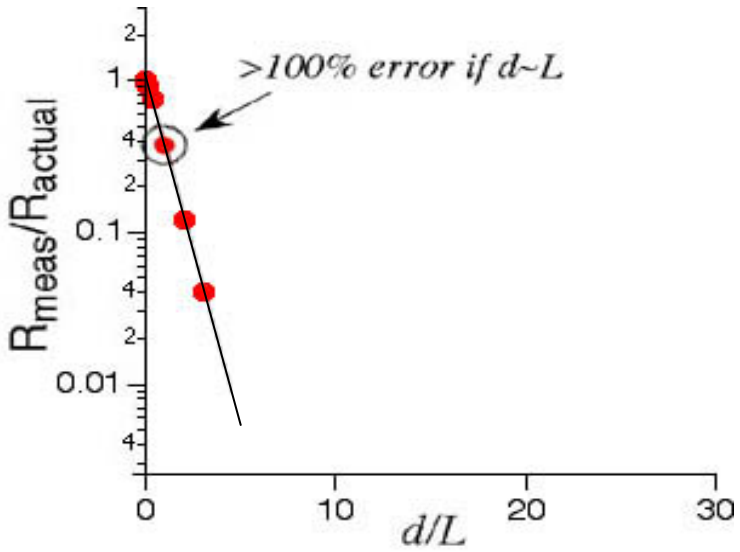

FEA Calculation

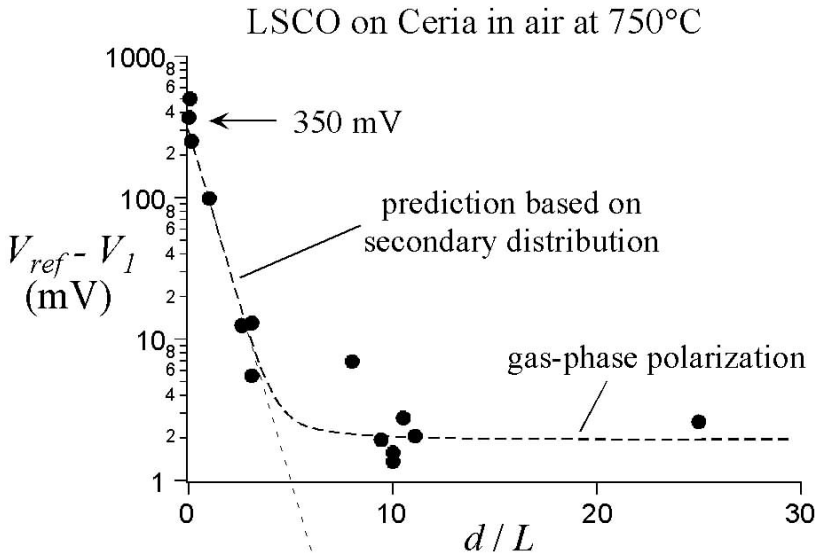

Measured Error

Error Includes Distortion of Impedance Spectra

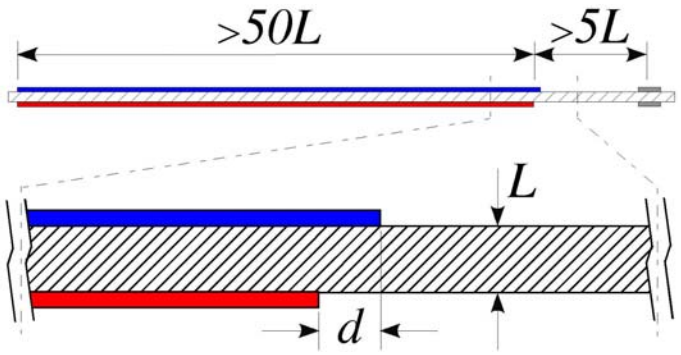

- "Cross-contamination" of WE and CE response.
- Distortion even with perfect electrode alignment.
- Impossible to avoid with thin cells having 1-D geometry.

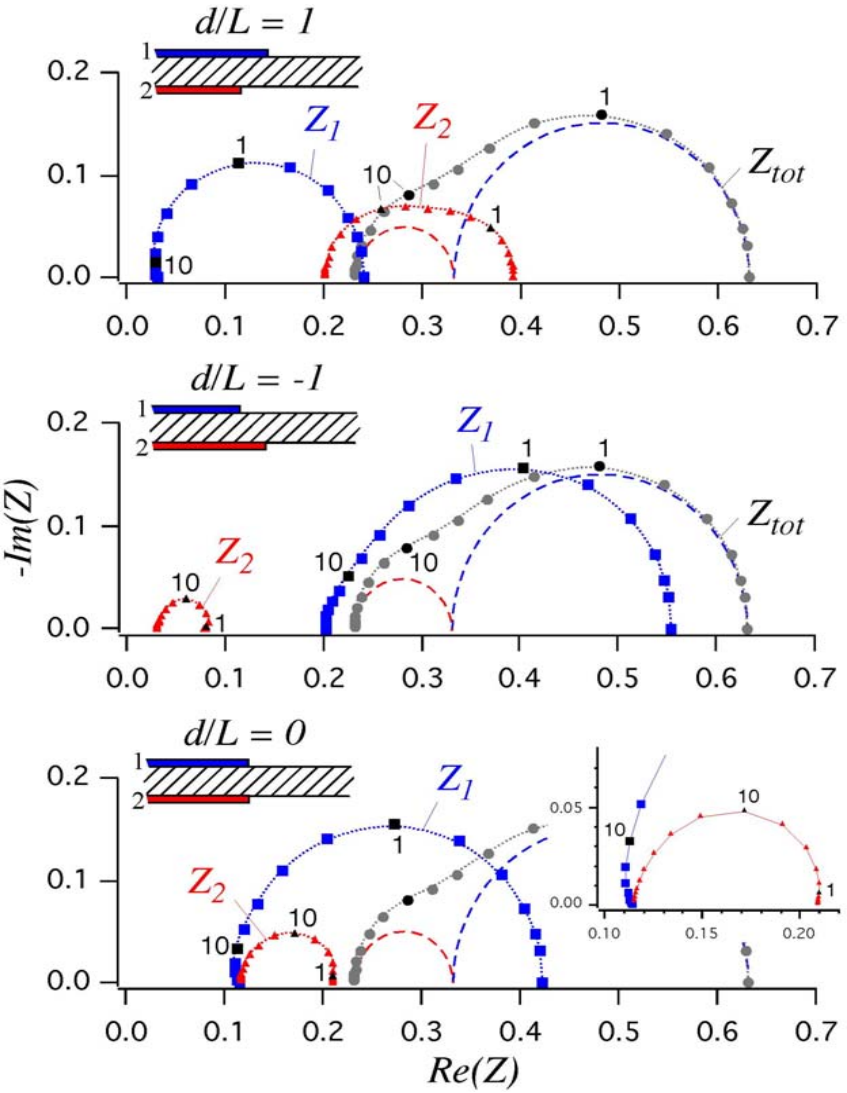

Theory behind a 2-D microelectrode

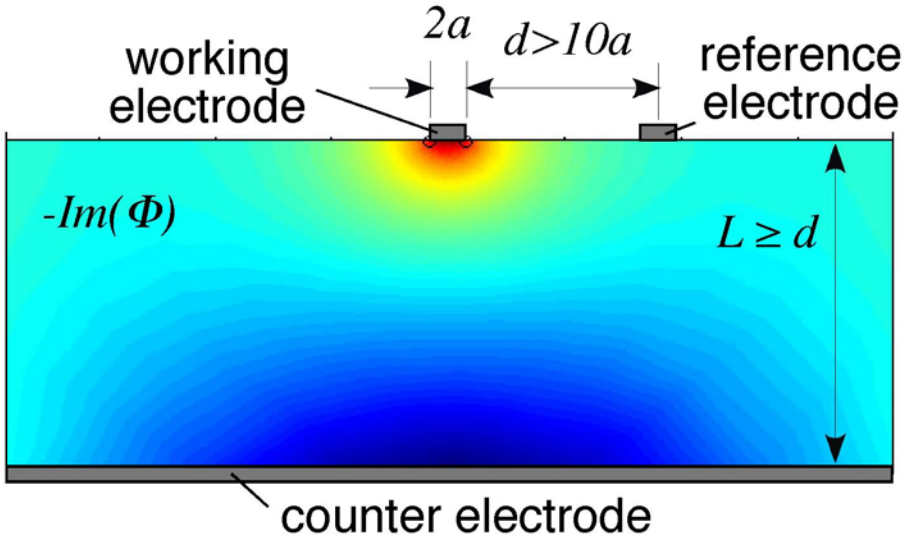

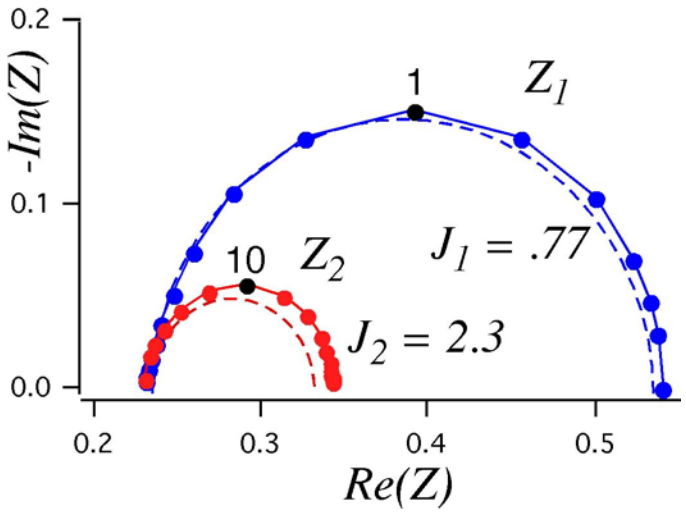

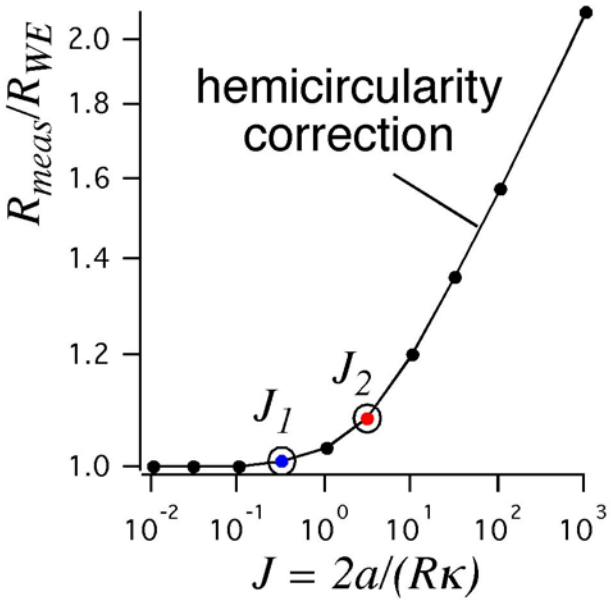

Potential benefits:

- High frequency isolation of WE.
- Representative materials.
- Ability to test at high bias.
- Reduced IR and inductive effects.
- Multiplicity through miniaturization.

Two approaches to 2-D “strip” microelectrode

Full Mask

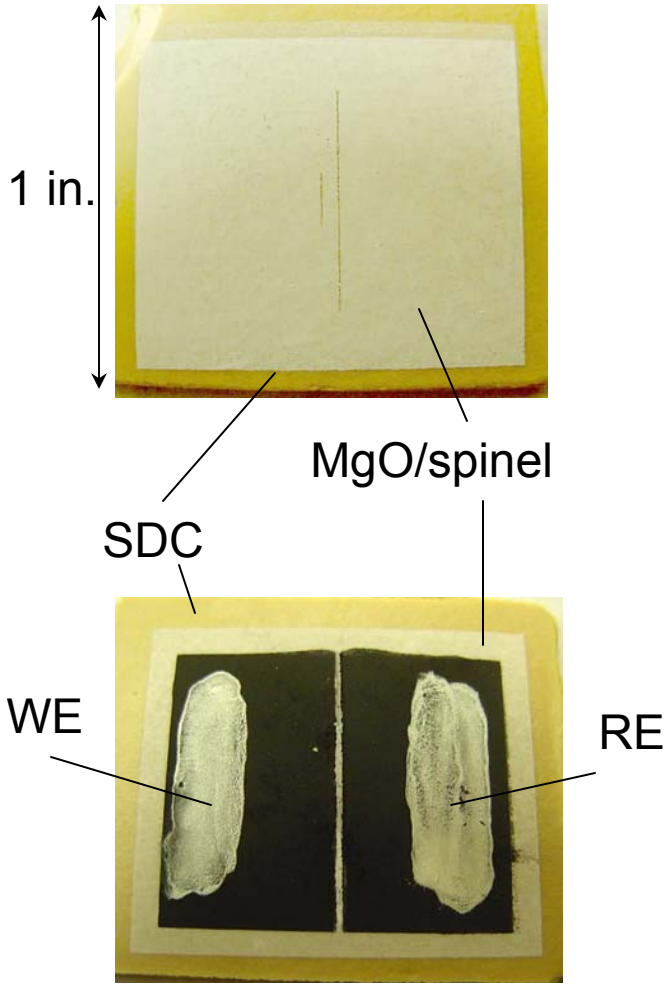

Partial Mask

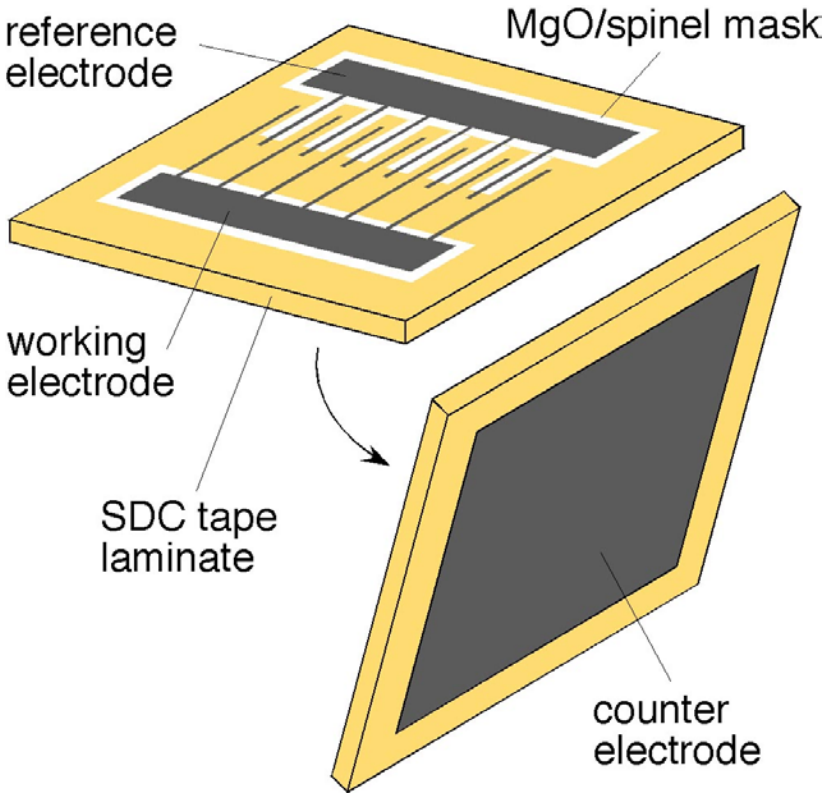

Verification of Microelectrode Half-cell Measurements

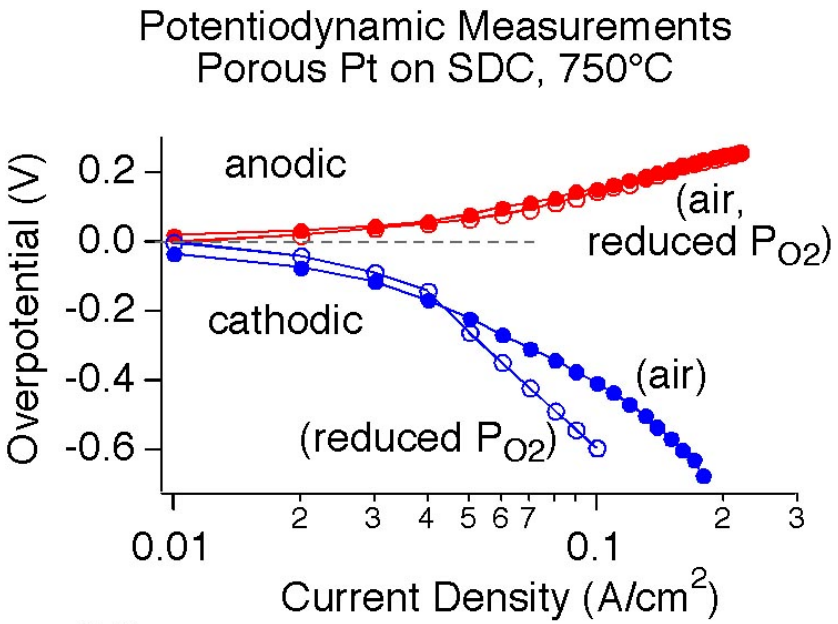

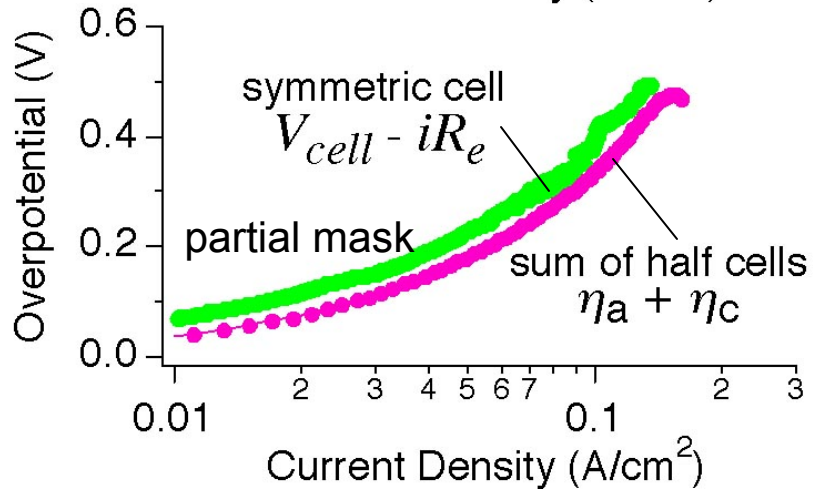

Procedure:

1) Measure $V(i)$ characteristics of microelectrode.
2) Subtract iR losses (based on impedance).
3) Add anode and cathode overpotentials.
4) Compare to $V(i)$-iR for a full-sized symmetric cell having the same electrodes.

Conclusions:

- 2-D microelectrodes can be quantitative.
- For Pt, measured iR losses match calculation based on measured geometry.
- Accuracy requires good lateral current distribution (Pt).

Microelectrodes not yet quantitative for perovskite electrodes

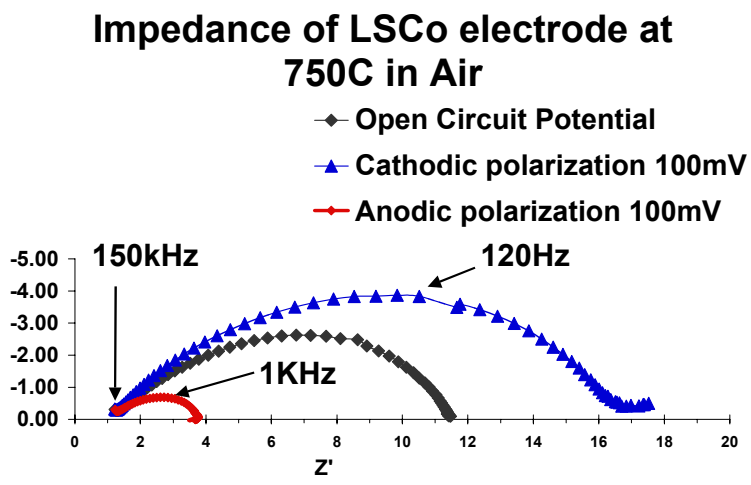

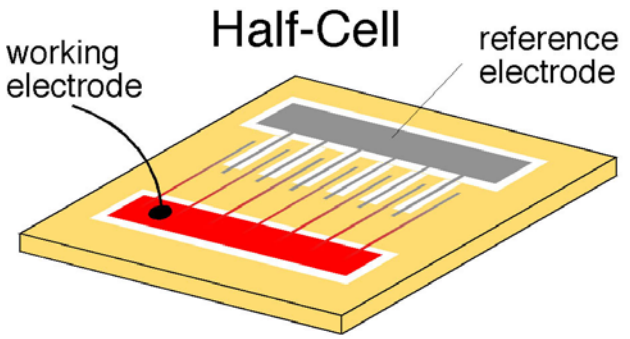

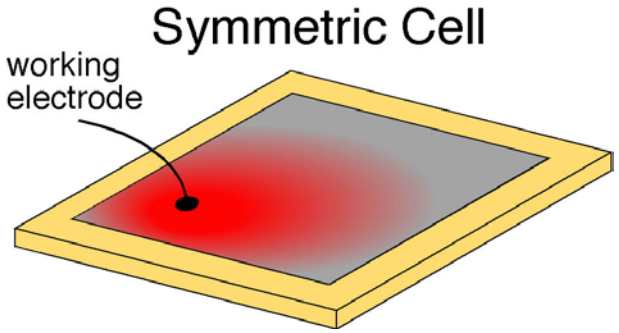

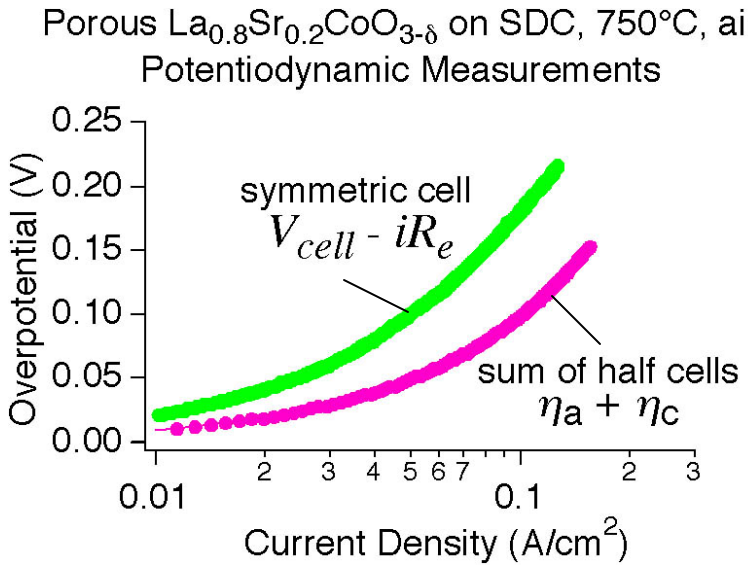

- Microelectrodes reveal qualitative differences b/t cathode and anode.
- Technique not yet quantitative due to poor lateral current distribution.

Current Status/Future Work

Partial Mask

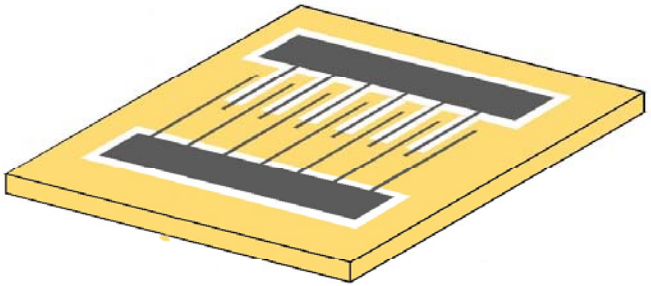

Full Mask

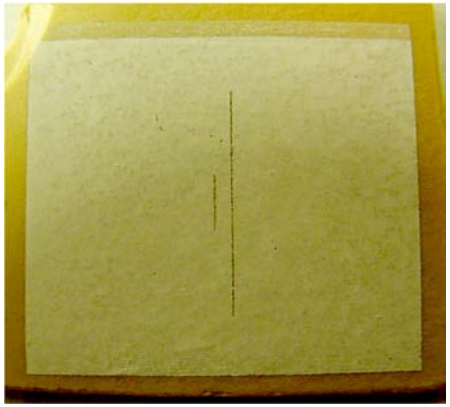

- To apply without correction factors, perovskites require a *full mask* config.
- It has proven difficult to produce thin, defect-free masks. Issues encountered:
  - mask porosity, thickness
  - expansion/adhesion of mask
  - electrolyte defects
- Current approach: 2 parallel paths
  - hybrid design with thick mask and metallic (Pt or Ag) bus.
  - thinner, screenprinted masks based on nanopowders.

What are harmonics, and why measure them?

$$V = V_0 + \left(V_1 e^{i\omega t} + V_1^* e^{-i\omega t}\right) + \left(V_2 e^{2i\omega t} + V_2^* e^{-2i\omega t}\right) + \ldots$$

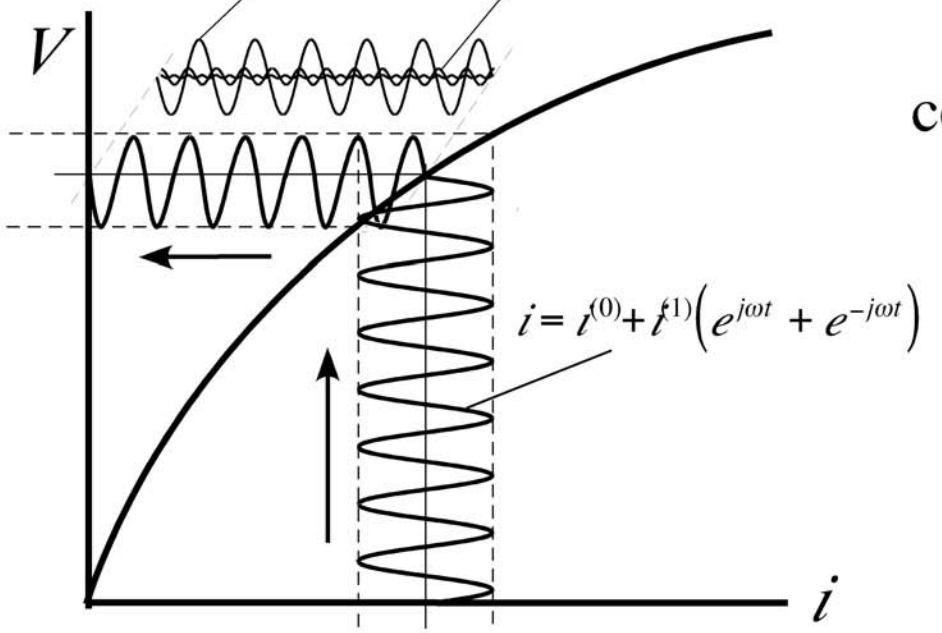

$\cos(\omega t)$ $\cos(\omega t)$ $\cos^2(\omega t)$

$$\frac{\partial c}{\partial t} = \frac{\partial^2 c}{\partial y^2} - v\frac{\partial c}{\partial y}$$

$$\cos^2(\omega t) = \frac{1}{2} + \frac{1}{2}\cos(2\omega t)$$

- All nonlinear systems generate responses at multiples of the excitation frequency (harmonics).
- The magnitude, sign, and phase of the harmonics are highly sensitive to the details of the underlying physics.

Types on nonlinear harmonic measurements

Nonlinear Electrochemical Impedance Spectroscopy (NLEIS)

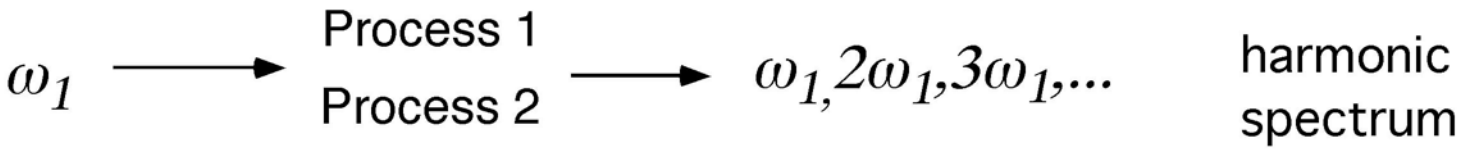

Electrochemical Frequency Modulation (EFM)

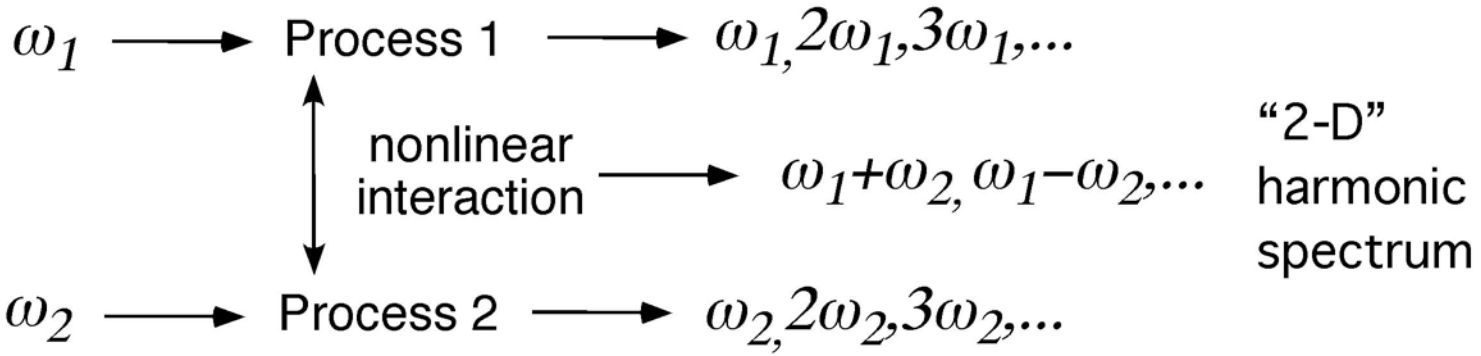

Our apparatus for NLEIS and EFM measurements

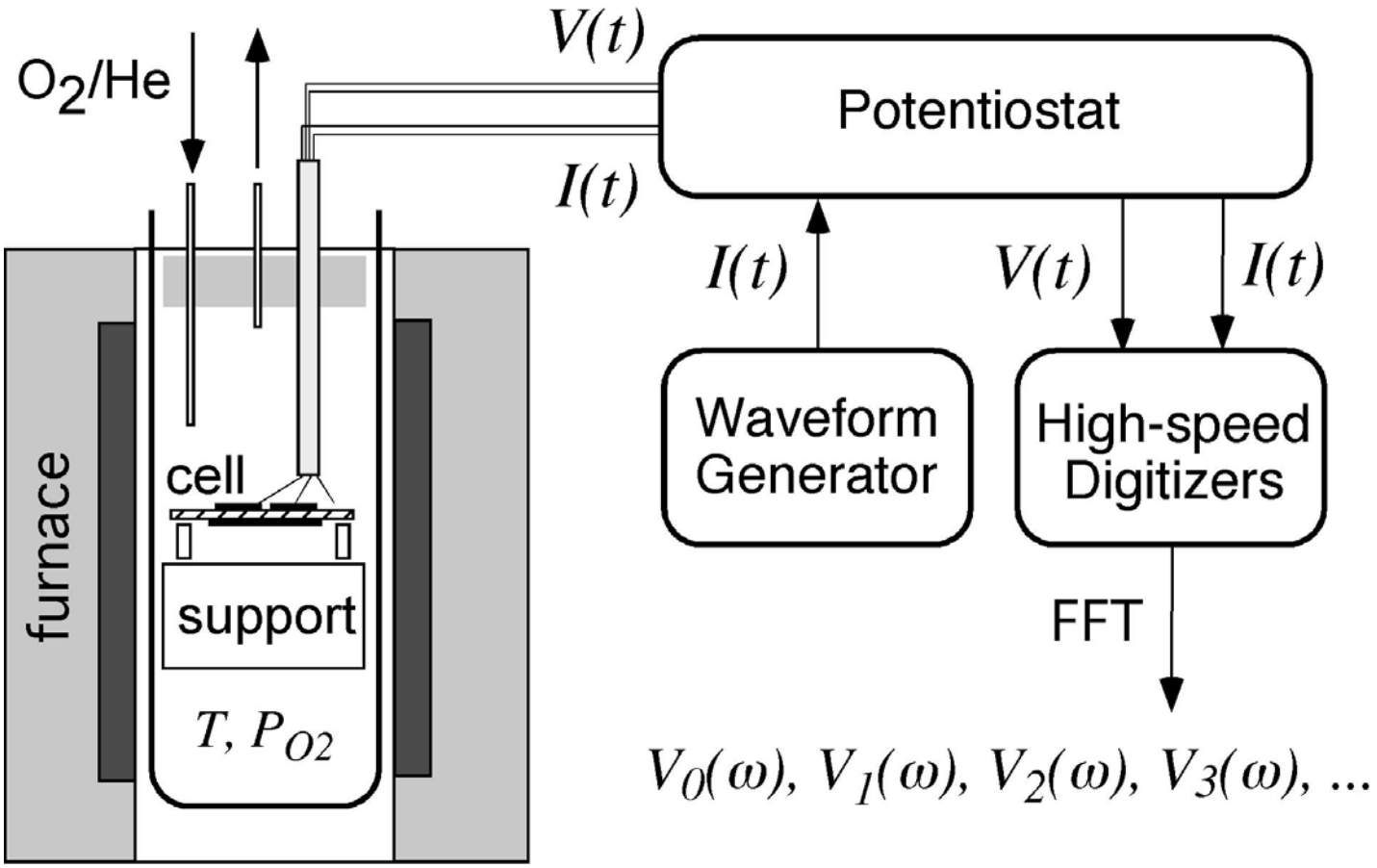

How NLEIS Data is Processed

example: LSF/ceria/LSF cell at 750°C in air (10 Hz)

Time-domain data

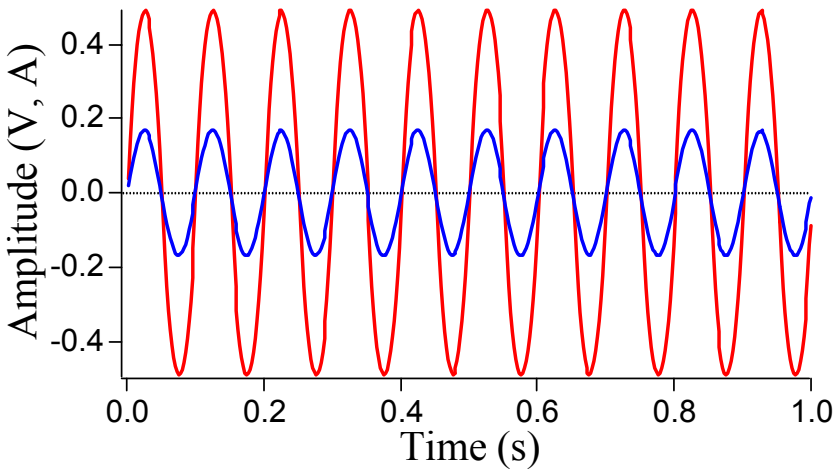

Gaussian Apodization

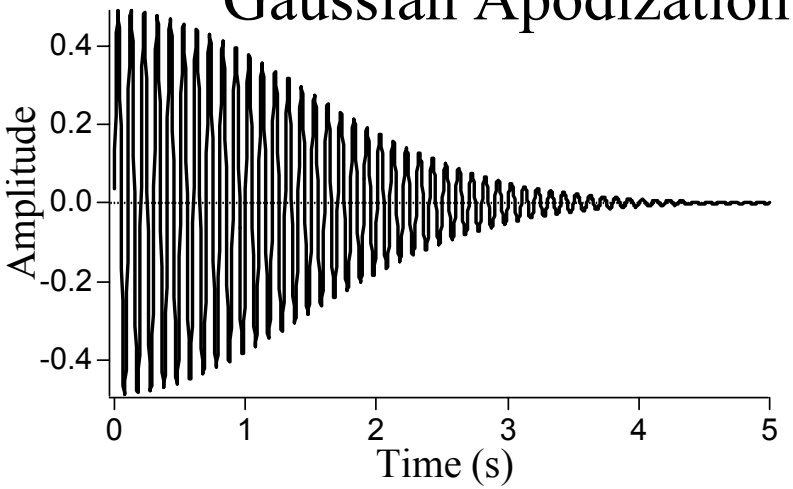

Current FFT (magnitude)

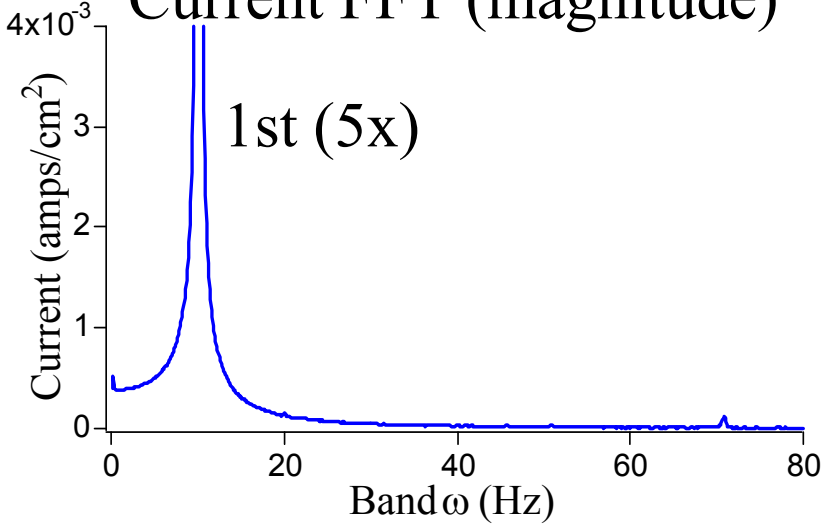

Voltage FFT (magnitude)

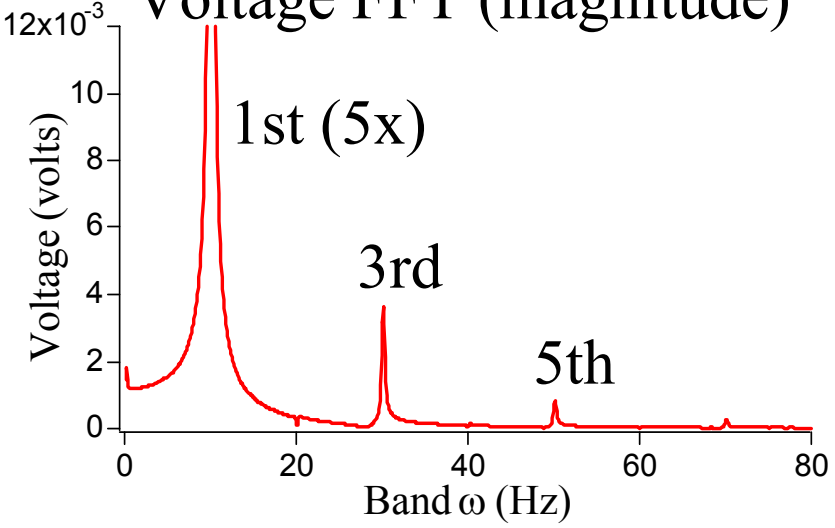

Voltage Signal Involves both Amplitude and Phase Shift

$$V(\alpha,\omega_0,t) = e^{-\frac{\omega_1^2 t^2}{4}} \sum_{k=1}^{\infty} \overline{V}_k(\alpha,\omega_0) e^{jk\omega_0 t} + \overline{V}_k^*(\alpha,\omega_0) e^{-jk\omega_0 t} \qquad \overline{V}_k = \hat{V}_k + j\tilde{V}_k$$

FFT

$$\mathrm{Re}\left(\overline{V}(\alpha,\omega_0,\omega)\right) = \sqrt{2}\sum_{k=1}^{\infty} \hat{V}_K(\alpha,\omega_0) \frac{e^{-\frac{(\omega \mp k\omega_0)^2}{\omega_1^2}}}{\omega_1} - \tilde{V}_K(\alpha,\omega_0) \frac{e^{-\frac{(\omega \mp k\omega_0)^2}{\omega_1^2}}}{\omega_1} erfi\left[\frac{\omega \mp k\omega_0}{\omega_1}\right]$$

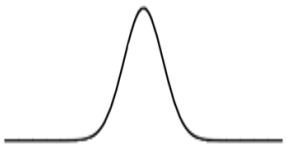

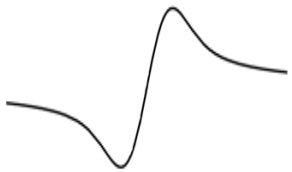

Complex Fourier Transform of Voltage Signal:

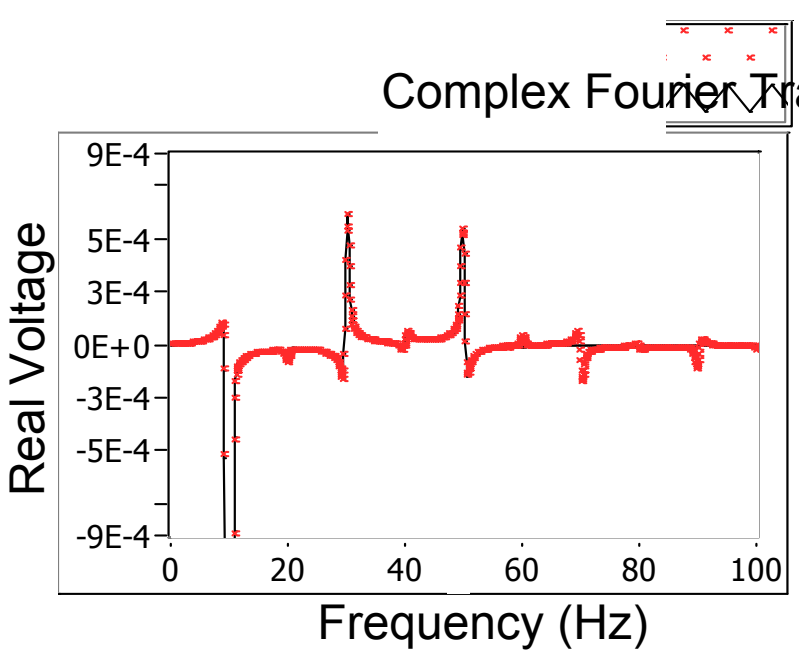

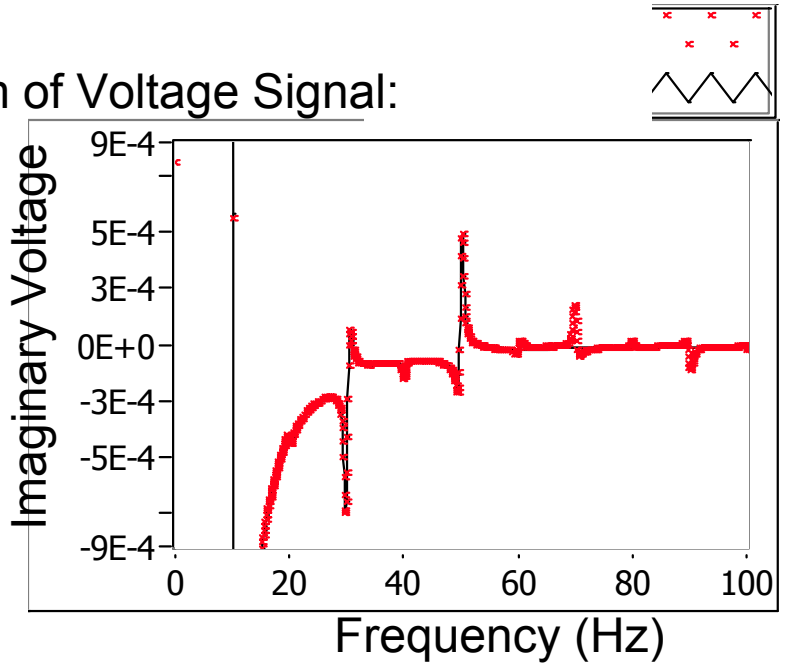

Gaussian Fit to Determine Precise Magnitude and Phase

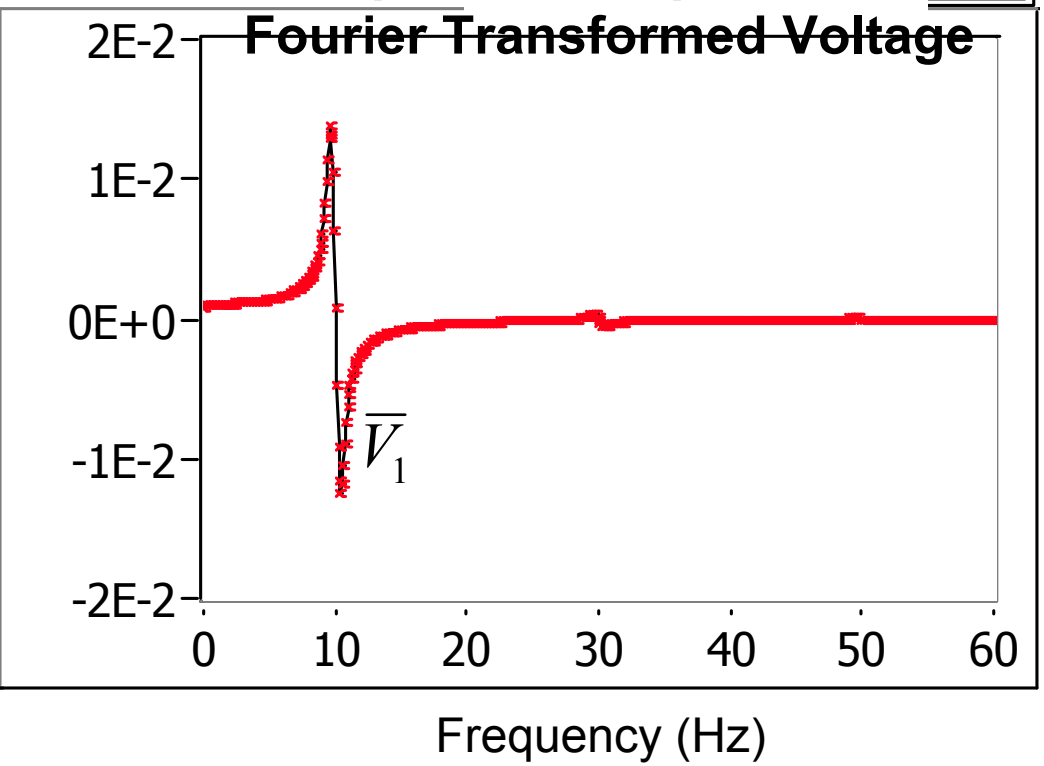

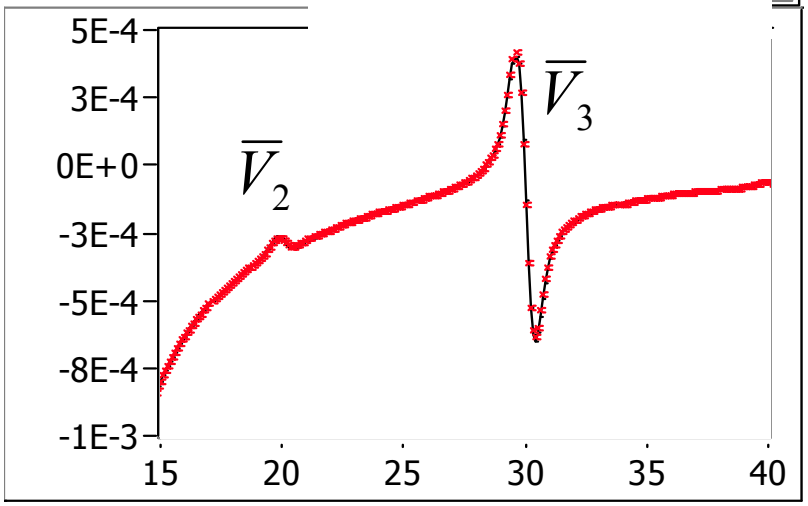

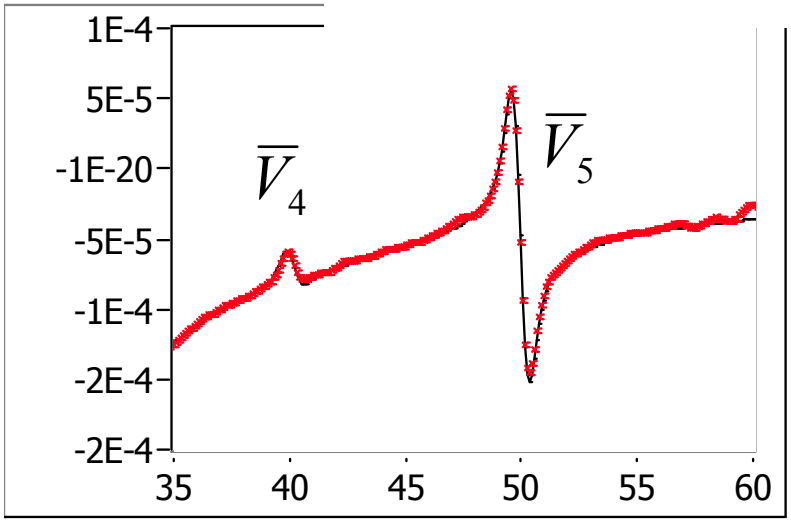

Power Series Expansion of Harmonic Response

$$\overline{V}_1(\alpha,\omega_0) = \alpha\overline{V}_{1,1}(\omega_0) + \alpha^3\overline{V}_{1,3}(\omega_0) + \alpha^5\overline{V}_{1,5}(\omega_0)$$

$$\overline{V}_3(\alpha,\omega_0) = \alpha^3\overline{V}_{3,3}(\omega_0) + \alpha^5\overline{V}_{3,5}(\omega_0)$$

Least Squares Fit

$$\overline{V}_k = \hat{V}_k + j\tilde{V}_k$$

$\hat{V}_k$ = Real Part of the Response

$\tilde{V}_k$ = Imaginary Part of the Response

First Harmonic:

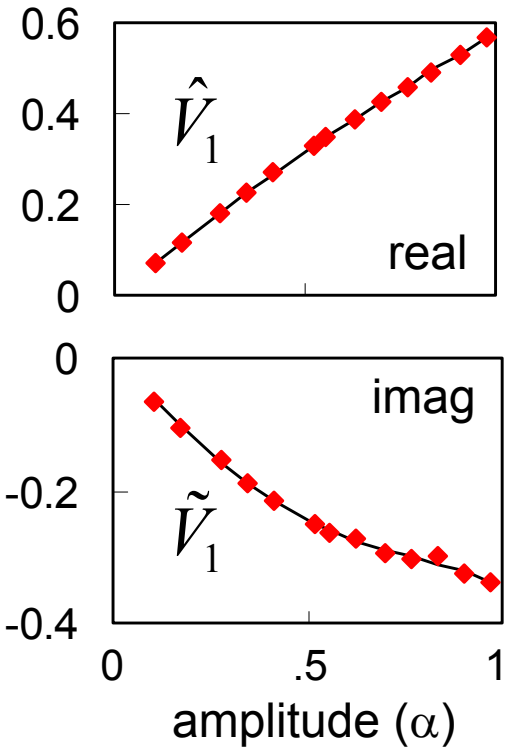

Third Harmonic:

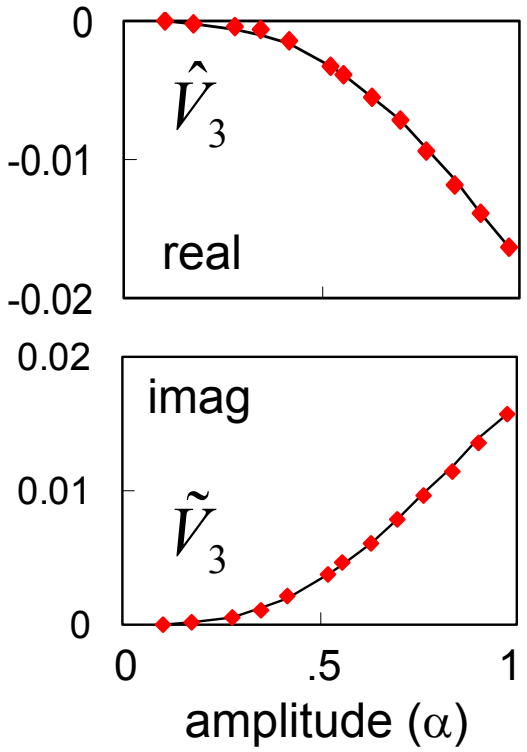

Harmonic Spectra $\overline{V}_{k,l}(\omega)$ of $La_{0.8}Sr_{0.2}CoO_{3-\delta}$ on SDC at 750°C in air

Bode Plots

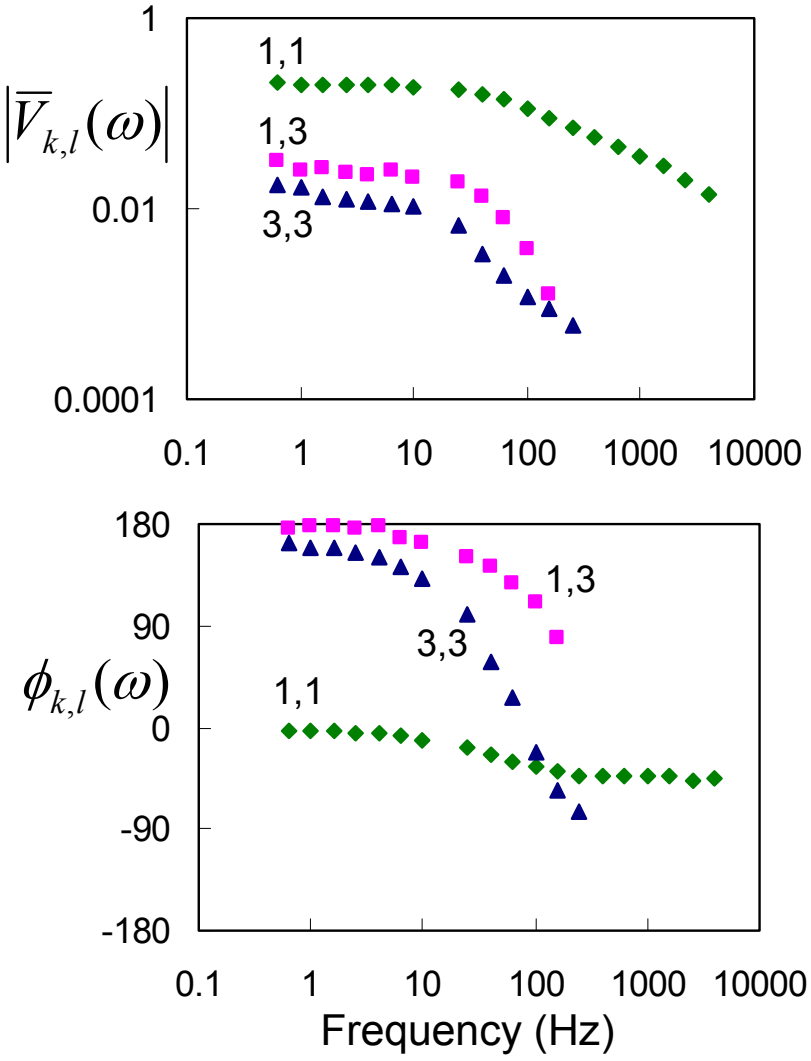

Nyquist Plots

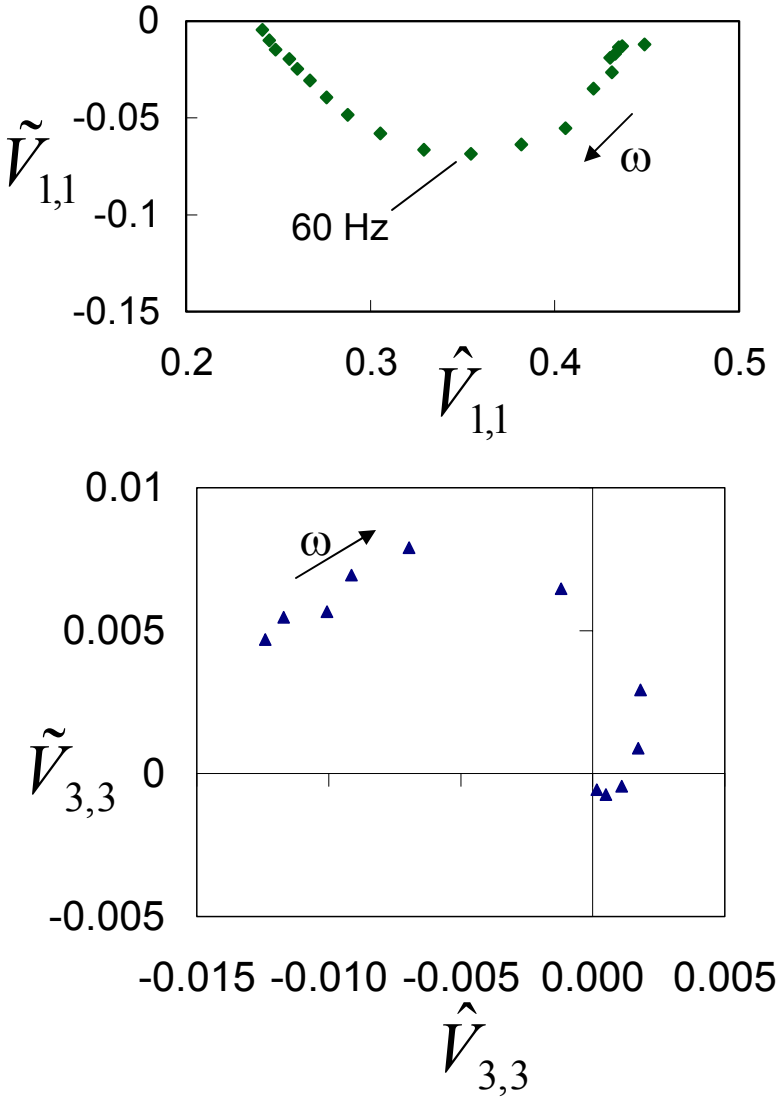

Extending existing models to the nonlinear regime

Possible reaction pathways for oxygen reduction:

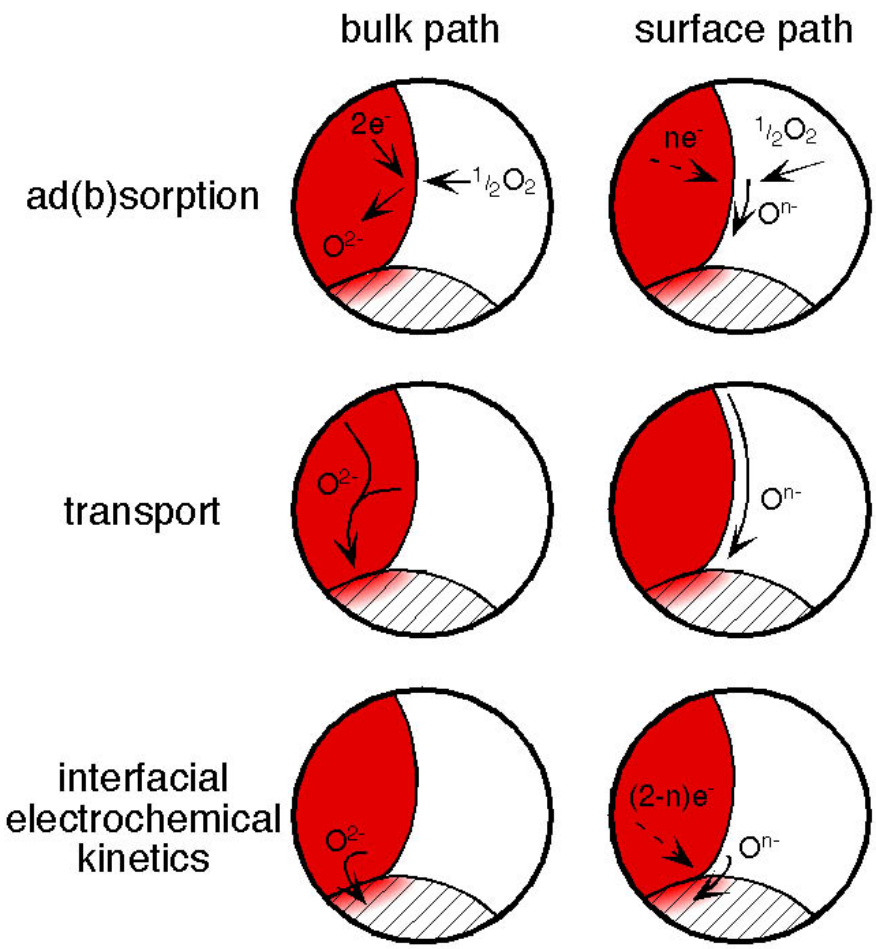

1-D model assuming a bulk path. (Adler, Lane & Steele, 1996)

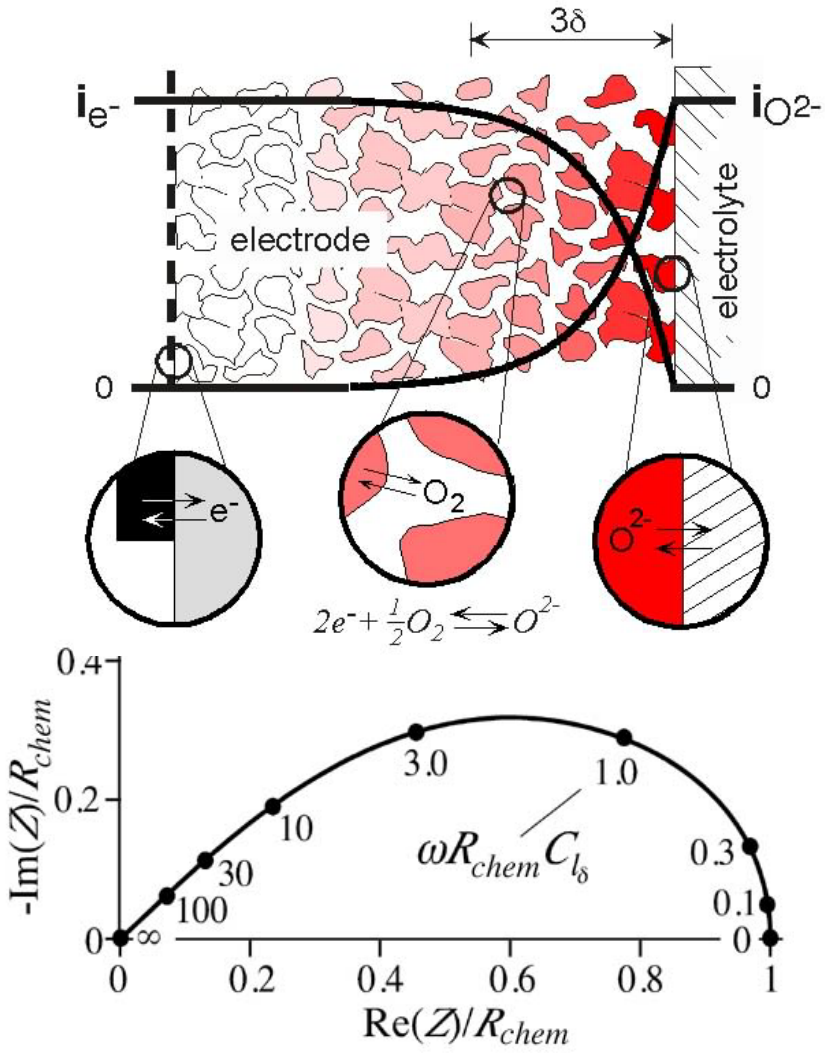

Extending existing models to the nonlinear regime

- Questions to be tested using the model:
  - Does the nonlinear response of LSC on SDC obey a bulk pathway model?
  - Is the solid-solid interface at equilibrium, as implied by the linear response?
  - What is the rate expression and mechanism of oxygen ad(b)sorption?

- Modeling assumptions:
  - 1-D geometry with average microstructural parameters.
  - Nonstoichiometry and diffusion based on bulk materials properties.
  - Interfacial charge-transfer based on Butler-Volmer rate equations.
  - O_2 reduction involves a single rate-determining step:

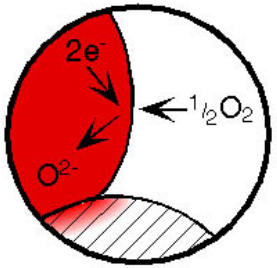

$$r = k\left(\frac{\left(P_{O_2}{}^{gas}\right)^n}{\left(P_{O_2}{}^{Solid}\right)^m} - \frac{\left(P_{O_2}{}^{Solid}\right)^{n-m+q}}{\left(P_{O2}{}^{gas}\right)^q}\right)$$

- Solution method:
  - Dual expansion of governing equations in a Fourier/power series.
  - Numerical formulation and solution using finite element analysis (FEMLAB).

Adsorption-limited O_2 exchange

$$rds: O_2^{(gas)} + 2s \leftrightarrow 2O^{(ads)}$$

$$r = k\left(\frac{\left(P_{O_2}{}^{gas}\right)^1}{\left(P_{O_2}{}^{Solid}\right)^{1-n}} - \left(P_{O_2}{}^{Solid}\right)^n \right)$$

$$(\text{shown}: \; n = 0.5)$$

- Model consistent with measured 1st harmonic (Gerischer), including -45° phase angle at high frequencies.
- Loss of higher harmonics (linearity) at high frequency confirms absence of polarization at the solid-solid interface.
- Sign and magnitude of harmonics at low frequency are not consistent with adsorption-limited O_2 exchange.

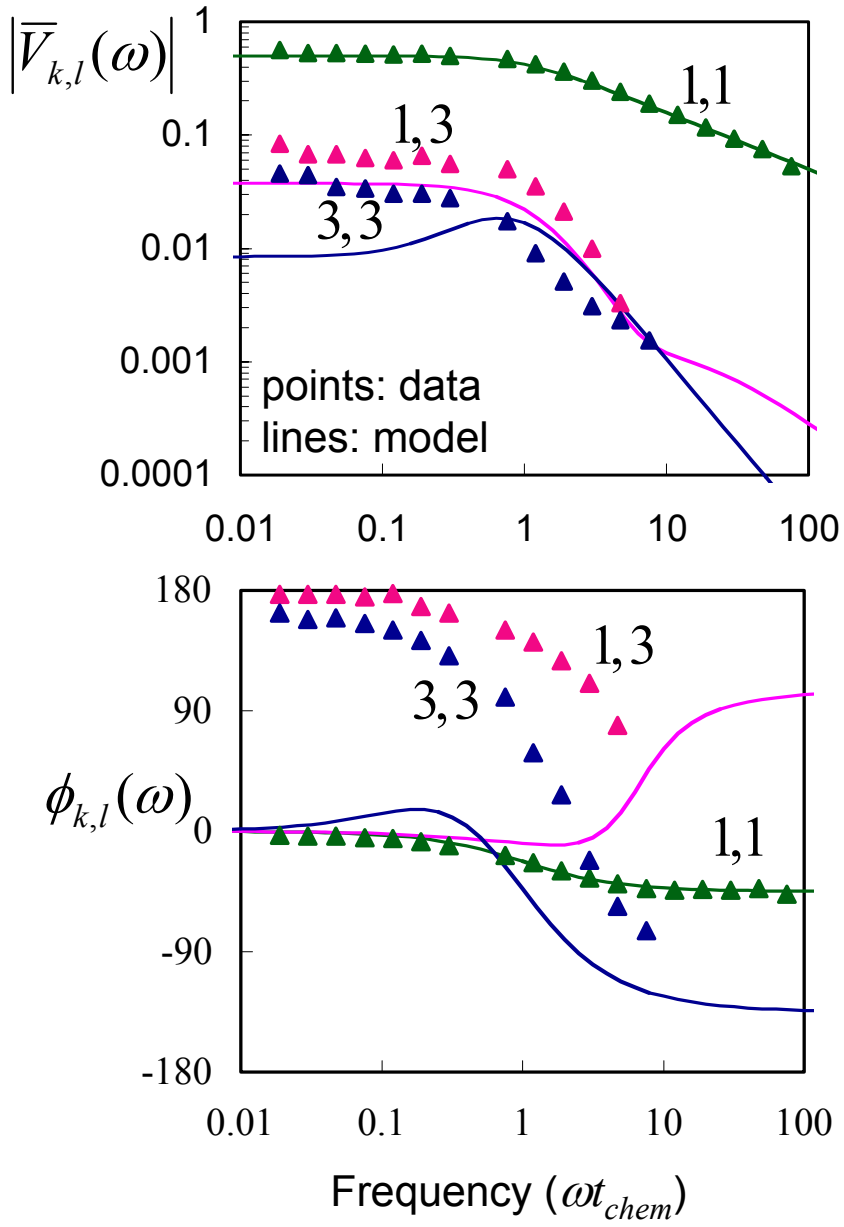

Incorporation-limited O_2 exchange

$$rds: O^{(ads)} + V_O^{\bullet\bullet} + 2e^- \leftrightarrow 0$$

$$r = k\left(\left(P_{O_2}{}^{gas}\right)^n - \left(P_{O_2}{}^{Solid}\right)^n\right)$$

$$(\text{shown}: \; n = 0.5)$$

- Model degenerate with previous model for the first harmonic.
- Symmetric rate expression results in nullifications (sign flips) in the higher harmonics, not present in the data.
- Sign and magnitude of harmonics at low frequency are not consistent with incorporation-limited O_2 exchange.

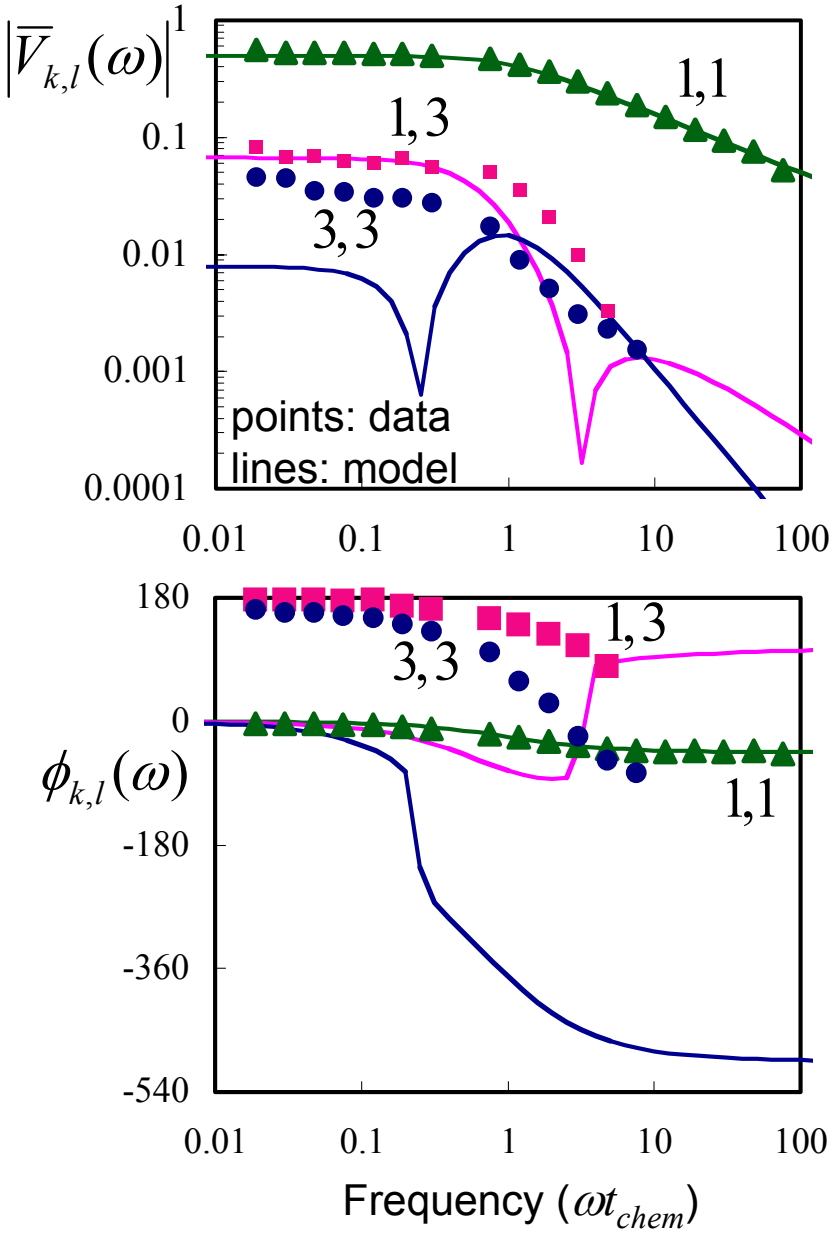

Empirically-derived rate

$$r = k\left(\frac{\left(P_{O_2}^{\ gas}\right)^{1}}{\left(P_{O_2}^{\ Solid}\right)^{93}} - \frac{\left(P_{O_2}^{\ Solid}\right)^{1.5}}{\left(P_{O_2}^{\ gas}\right)^{1.47}}\right)$$

$$rds : (\text{none possible})$$

- Model degenerate with other models for the first harmonic; but better agreement in all harmonics over entire spectrum.
- Predicted weak exchange rate ($\sim P_{O_2}^{0.1}$) is consistent with weak dependence previously observed in r_0 *vs* P_{O2}.
- This rate expression very hard to justify based on a single rate-determining step, plus bulk diffusion (only).

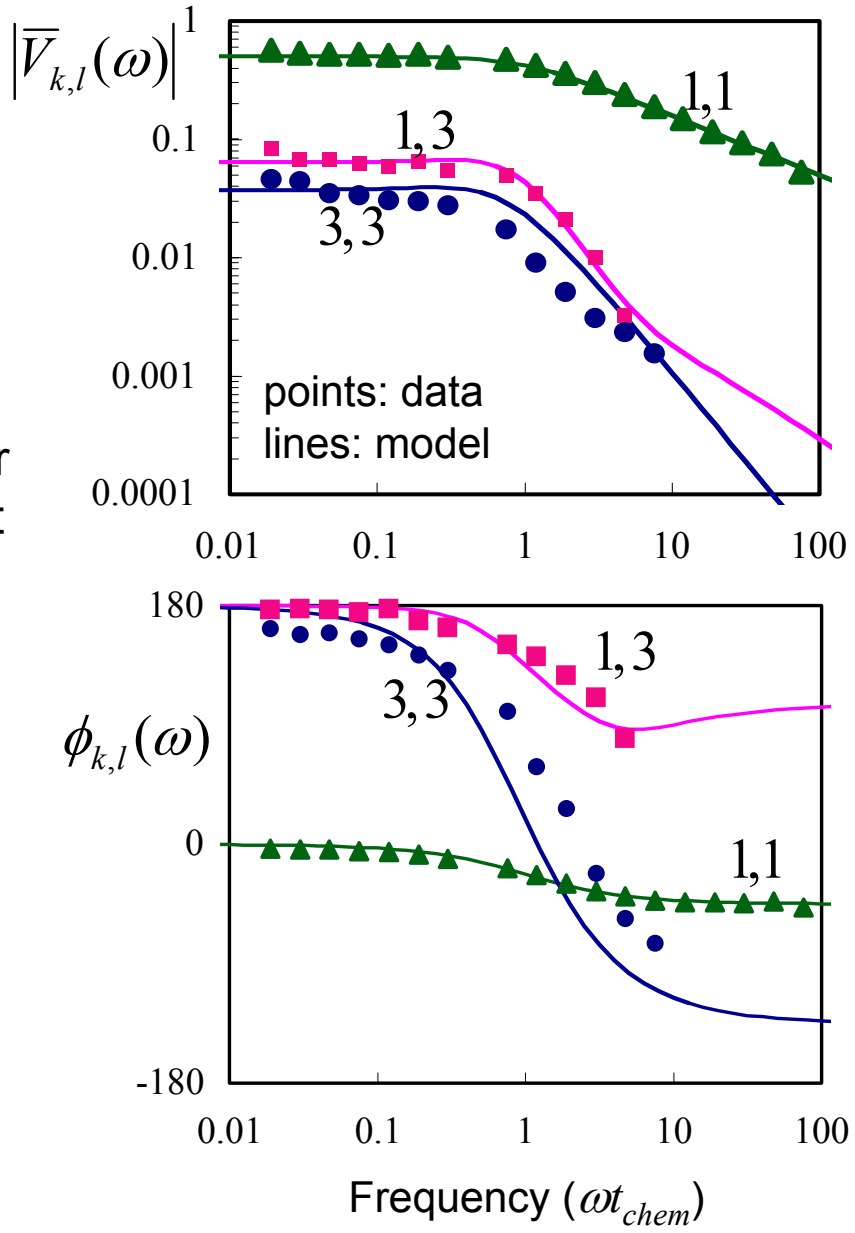

Conclusions

- Higher harmonics provide additional nonlinear information that *severely restricts* possible mechanisms underlying a.c. behavior.

- When fired at sufficiently high temperatures, LSC on SDC exhibits nearly zero resistance to charge-transfer at the solid-solid interface. Polarization is due to chemical dissociation and transport.

- For $La_{0.8}Sr_{0.2}CoO_{3-\delta}$ at 750°C in air, higher harmonics do not seem consistent with a bulk path involving a single *rds* for O_2 exchange. Possible explanations:
  - multiple rate-determining steps for O_2 exchange.
  - local morphological effects.
  - **parallel surface path** (favored explanation).

Current/Future Work (NLEIS)

- NLEIS measurements on dense thin-film perovskite electrodes, eliminating surface path.
- Measurements of LSCF porous electrodes over a wider range of temperature, P_{O2}, Sr content, surface area, and interfacial bonding.
- Measurements of 2nd and 4th harmonics (half cells).

Summary

- Microelectrodes potentially offer an easy, reliable vehicle for half-cell measurement and testing.
- NLEIS shows promise as a superior method for electrode analysis and characterization, with little additional experimental effort/time *vs*. EIS.